Int. J. Electrochem. Sci., 8 **(2013)** 7565 - 7580

International Journal of
ELECTROCHEMICAL
SCIENCE
www.electrochemsci.org

A Cubic Silsesquioxane Modified With Purpald®: Preparation, Characterization and a Voltammetric Application for Determination of Sulfite

Layciane Aparecida Soares[1], *Wang Yingzi*[2], *Tayla Fernanda Serantoni da Silveira*[1], *Daniela Rodrigues Silvestrini*[1], *Urquisa de Oliveira Bicalho*[1], *Newton Luiz Dias Filho*[1], *Devaney Ribeiro do Carmo*[1,*]

[1]Faculdade de Engenharia de Ilha Solteira UNESP – Univ. Estadual Paulista, Departamento de Física e Química, Av. Brasil Centro, 56 CEP 15385-000, Ilha Solteira, SP, Brazil. Fax: +55 (18) 3742-4868.
[2]Shanghai University, Department of Chemistry College of Science, Shangda Road, 99 Zip Code 200444, BaoShan District, Shanghai, China. Fax: (+86) 18801912699
[*]E-mail: docarmo@dfq.feis.unesp.br

Received: 4 April 2013 / *Accepted:* 11 May 2013 / *Published:* 1 June 2013

A novel composite formed by interaction of a octa(3-chloropropyl)octasilsesquioxane modified with Purpald®, and its subsequent reaction with silver and hexacyanoferrate (III) (AgHSP), was synthesized and initially characterized by Fourier transform infrared spectra (FTIR) and cyclic voltammetry. The cyclic voltammogram of the modified graphite paste electrode with AgHSP, showed one redox couple with formal potential $E^{\theta'}$=0.64V (*vs* Ag/AgCl, KNO_3, 1.0 mol L^{-1}; *v* = 20 mV s^{-1}), attributed to the $Fe^{2+}(CN)_6$/ $Fe^{3+}(CN)_6$ process. The redox couple presents an electrocatalytic response for determination of sulfite. The modified electrode showed a linear response from 7.0×10^{-5} to 1.0×10^{-3} mol L^{-1} with the corresponding equation Y(μA) = 18.05 + 29.983×10^{3} [sulfite], and a correlation coefficient of r=0.999. The method showed a detection limit of 0.115×10^{-4} mol L^{-1} with a relative standard deviation of ± 4% (*n* = 3) and amperometric sensitivity of 29.983×10^{-3}A mol L^{-1}. The modified electrode showed a excellent stability and good reproducibility during experiments.

Keywords: octa(3-chloropropyl)octasilsesquioxane, purpald, sulfite, graphite paste electrode, voltammetry

1. INTRODUCTION

Silsesquioxanes or spherosiloxanes are nanostructured materials which have the empirical formula $(RSiO_{1.5})_n$, where R can be a hydrogen or any organic group such as alkyl, methyl, aryl, vinyl,

phenyl, arylene or any organofunctional derivative thereof [1-5] and *n* is an integer number that can vary, in $n \geq 4$, but it is usually 6, 8 or 10 [4].

Polyhedral oligomeric silsesquioxanes (POSS) or silsesquioxanes with "cage" structures are also known as and are widely studied because of their well-defined and highly symmetric structure. The octahedral species (cubes), whose typical structure is $(RSiO_{1.5})_8$, that is, they hold 8 silicon atoms located at the vertices of its structure [3,5-7]. These nanostructured materials have diameters ranging from 1 to 3 nm and are considered the smallest possible silica based particles [2].

The chemical properties of these silsesquioxanes structures have been studied for over half a century [1,2]. The exponentially increase in the number of publications and patents related to preparation and application methods is quite evident and this is largely due to the structural similarities and electronic properties exhibited by the silanol groups demonstrated by silica. Thus, this ability to mimic the reactivity of silanol groups on the silica surface is responsible for major advances in understanding the physico-chemical properties of silsesquioxanes [1,8].

Polysilsesquioxanes are generally synthesized by hydrolytic condensation of the monomer $RSiX_3$ [3,8-11] where R is an organic group and X is -Cl, -OH, -OR (alkoxide) or OAc (acetoxy). The X groups can be hydrolyzed to form Si-OH reactive groups, which can then condense with the formation of bridges Si-O-Si [11,12]. The molecules used in the preparation of a silsesquioxane are relatively simple. The most used, for example, are tetraethoxysilane, methyltriethoxysilane and dimethyldietoxysilane [11], and the reaction product is a high molecular mass polymer.

The advantages of using POSS rather than other molecules, such as clays, carbon fibers and carbon nanotubes, is because they are much smaller and have a monodispersed size, low density, and are readily modified chemically to generate a series of reactive substituents to suit a particular application [4]. When organo or inorgano functionalized, silsesquioxanes can improve their chemical and physical properties [2,3,5], for instance, in the adsorption field they can be used to increase the sorptive capacity of metal ions in aqueous or organic solutions [13-15].

The derivatives of POSS can have a hybrid architecture (inorganic/organic) with an internal inorganic structure formed by silicon and oxygen, which is externally covered by organic substituents [16]. These materials are prepared by functionalization reactions in which the organic compound is bonded to the peripheral groups of POSS [17]. An important characteristic of the derivatives of POSS, is your advantage of, besides being chemically stable, being non-volatile, odorless materials, which do not cause environmental impacts [2].

The silsesquioxanes have a large number of applications, and this number increases when these structures are used as precursors in the formation of organic-inorganic hybrid materials [3,5]. The applications of these materials include electronic devices [2], biosensors [2,4,5], catalysts [2,3,8,16,18,19,20], electrocatalyst [21,22], electroactive and thin films [23,24], polymers [2,4], fuel cells [3], liquid crystals [3,4], optical fiber coatings [3], additives [3,25,26], optical devices [5], antibacterial and biocides [27] and silica interface precursors [11].

Electrodes chemically modified using silsesquioxane is uncomum are arousing great interest in the area of electrochemistry, due to easy preparation and by possibility of those materials act as power electrocatalysts [28,29].

Many ways of anchoring compounds electrochemically active in the surface have been investigated in order to shorten the distance between the sites of oxidation-reduction involved in electronic transfer reactions [30,31].

Based on our interest in developing modified electroactive hybrid composites for electroanalytical purposes, in this paper we present the preparation, preliminary characterization and voltammetric study of silver hexacyanoferrate (AgHCF) obtained by the interaction of the functionalized polyhedral oligosilsesquioxane with the 4-amino-3-hydrazino-5-mercapto-1,2,4-triazole, (SP), and respective interactions with AgHCF in two stages. At the first stage, the SA adsorbs Ag^+ and the second step the composite formed (AgSA) reacts with hexacyanoferrate (III) forming a new composite (AgHSA).

4-amino-3-hydrazino-5-mercapto-1,2,4-triazole, also known as Purpald® (Figure 1(B)), is a chromogenic agent that is widely used in the determination of aldehyde. Purpald® possesses S–C–N linkages and displays potential ligands for metal complexes that may also be biologically active just like some other amine- and thione-substituted trizoles [32]. Thus, the interest in using this binder is due to the fact that it has NH_2 sites conducive to organofunctionalization with octa-(3-chloropropyl)silsesquioxane , as well as S groups that are excellent active sites for the adsorption of metal ions. Thus the S will serve as chelation of Ag^+ ions. The idea is that AgHSA can provide a good electron shuttle between the substrate (i.e. enzyme) and the electrode. Additionally, the presence of silsesquioxane, which is an electron acceptor [19], can provide stabilizing microenvironment around the substrate. After rigorous voltammetric studies, the composite was tested in the electrocatalytic determination of sulfite (SO_32-). Sulfite are used as preservatives in the food industry to prevent oxidation and to help preserve vitamin C [36]. The toxicity of sulfites can produce asthmatic, mutagenic, and co carcinogenic effects [34,35]. Due to the toxicity, oxidizing and carcinogenic properties of this ion, the detection of sulfite is very important; mainly from environmental, biological and industrial point of view.

2. EXPERIMENTAL

2.1. Reagents and solutions

All reagents and solvents were of analytical grade (Alpha Aesar, Merck or Aldrich) and were used as purchased. All solutions and supporting electrolytes were prepared using Milli-Q water. The 0.1 mol L^{-1} NaOH and HNO_3 solution was used to adjust the different pHs.

2.2. Techniques

2.2.1. Fourier transform infrared spectra

Fourier transform infrared spectra were recorded on a Nicolet 5DXB FT-IR 300 spectrometer. Approximately 600 mg of KBr was ground in a mortar with a pestle, and sufficient solid sample was

ground with KBr to make a 1wt % mixture to produce KBr pellets. After the sample was loaded, the sample chamber was purged with nitrogen for a minimum of 10 min. prior to data collecting. A minimum of 32 scans was collected for each sample at a resolution of 4 cm^{-1}.

2.2.2. Electrochemical Measurements

Cyclic voltammograms were performed using the Microquimica (MQP1- PGST) potentiostat. The three electrode systems used in these studies consisted of a modified working electrode (graphite paste electrode) an $Ag/AgCl_{(s)}$ reference electrode, and a platinum wire as the auxiliary electrode. The measurements were carried out at 25°C.

2.3. Synthesis of octa-(3-chloropropyl)silsesquioxane (S)

For the synthesis of octa-(3-chloropropyl)silsesquioxane (S) (Fig. 1A) a procedure described in the literature was followed with [27].

800 ml of methanol, 27 ml of hydrochloric acid (HCl) and 43 mL of 3-chloropropyliltriethoxysilane were added into a round bottom flask of 1000 mL. The system was kept under constant stirring at room temperature for 6 weeks. The solid phase was separated by filtration in a sintered plate funnel, yielding a white solid, octa-(3-chloropropyl)silsesquioxane (S), which was then oven dried at 120 ºC for 4 hours. Fig. 1 illustrates a representative scheme of this synthesis.

2.4. Functionalization of octa-(3-chloropropyl)silsesquioxane with Purpald®

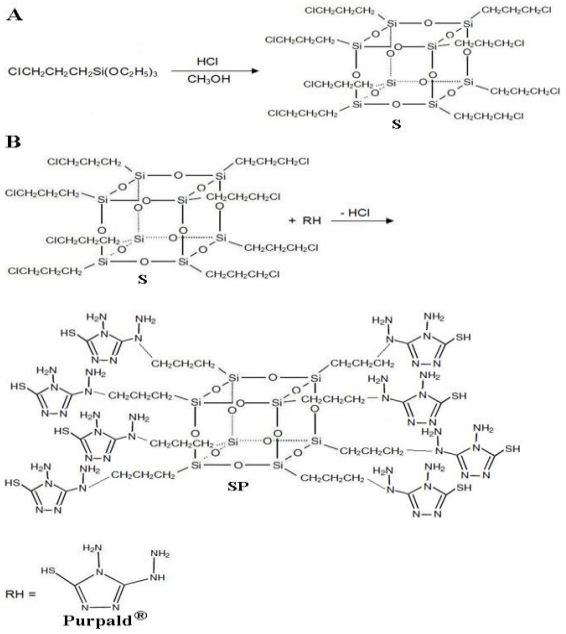

Figure 1. (A) Schematic representation of the preparation of octa-(3-chloropropyl)silsesquioxane [36-adapted] and (B) organofunctionalization of octa-(3-chloropropyl) silsesquioxane (S) with the modifying agent Purpald®.

The functionalization of octa-(3-chloropropyl)silsesquioxane (S) (Fig. 1B) was performed in a 3-neck flask of 500 mL containing 10 g (9.7×10^{-3} mol) of S, previously dried at 100°C for 2 hours (8.7×10^{-2} mol) of Purpald® and approximately 200 mL of dimethylformamide (DMF). The mixture was refluxed at 160 °C with constant stirring for 96 hours. Then the solid plate was separated in a sintered funnel and washed in a Soxhlet extractor with DMF for 48 hours. The material obtained was oven dried 100 °C for 4 hours and described as SP.

2.5. Reaction of Silver and Hexacyanoferrate with SP to form AgHSP

The AgHSP composite were prepared as follows: 1.0 g of SP was added to 25 mL of a solution of 1.0×10^{-3} mol L^{-1} silver nitrate. The mixture was stirred for 1h at room temperature. The solid phase was then filtered and washed thoroughly with deionized water. The material resulting from this first phase were oven dried at 70ºC and designated as AgSP. In the second stage, the AgSP was added to a solution of 1.0×10^{-3} mol L^{-1} of potassium hexacyanoferrate (III), and the mixture was stirred for 1h at room temperature and then the solid was thoroughly filtered, washed with deionized water and dried at 70ºC. The materials resulting from this stage were described by AgHSP.

2.6. Preparation of Chemically modified carbon paste electrodes

The chemically modified carbon paste electrodes were prepared by mixing the modified silsesquioxane (20mg), graphite powder (80 mg), and nujol oil (25 μL). The electrode body was fabricated from a glass tube of i.d. 3 mm and height of 14 cm, containing graphite paste. A copper wire was inserted through the opposite end to establish electrical contact. After the mixture had been homogenized, the modified paste was carefully positioned on the tube tip to avoid possible air gaps, which often enhances electrode resistance. The external surface of the electrode was smoothed on soft paper. A new surface can be produced by scraping out the old surface and replacing the carbon paste.

3. RESULTS AND DISCUSSION

Fig. 2 shows the vibrational spectrum of all synthesized materials. Fig. 2D shows the functionalized SP material, which showed absorption bands that are characteristic of the starting materials S and Purpald® such as the bands at ~1120 cm^{-1} relative to Si-O-Si (υ Si-O-Si) for the asymmetric stretch corresponding to the cage shaped structure of silsesquioxane (Fig. 2A), showing that the cubic structure was maintained, another at ~2959 cm^{-1} for the bonding deformation, and another at C–H (υ C–H) and another at ~ 2980 cm^{-1} ascribed to the vibration of the S–H bond (υ S-H), and the intense bandwidth is attributed to deformation O-H of the molecules H_2O (υ O-H). The bands between 1345 and 1700 cm^{-1} (Fig. 2D) were attributed to the vibrations and deformations of the Purpald® ring [37]. Most of the absorption peaks of S (Fig. 2A) and Purpald® (Fig. 2B) are overlapped, and the FTIR spectra of SP composite are similar with that pure S, but the low observed intensity

signal of the band at 590 cm^{-1} related to the C-Cl vibrations confirm the organofunctionalization of S with Purpald® (SP).

As an application of this novel composite, SP was firstly reacted with Ag^{+}, and then with hexacyanoferrate (III) to form (AgHSP), however the AgHSP was obtained in two stages (item 2.2). The success of synthesis was verified by vibrational spectroscopy (FTIR) as illustrated by Fig. 2C and 2E.

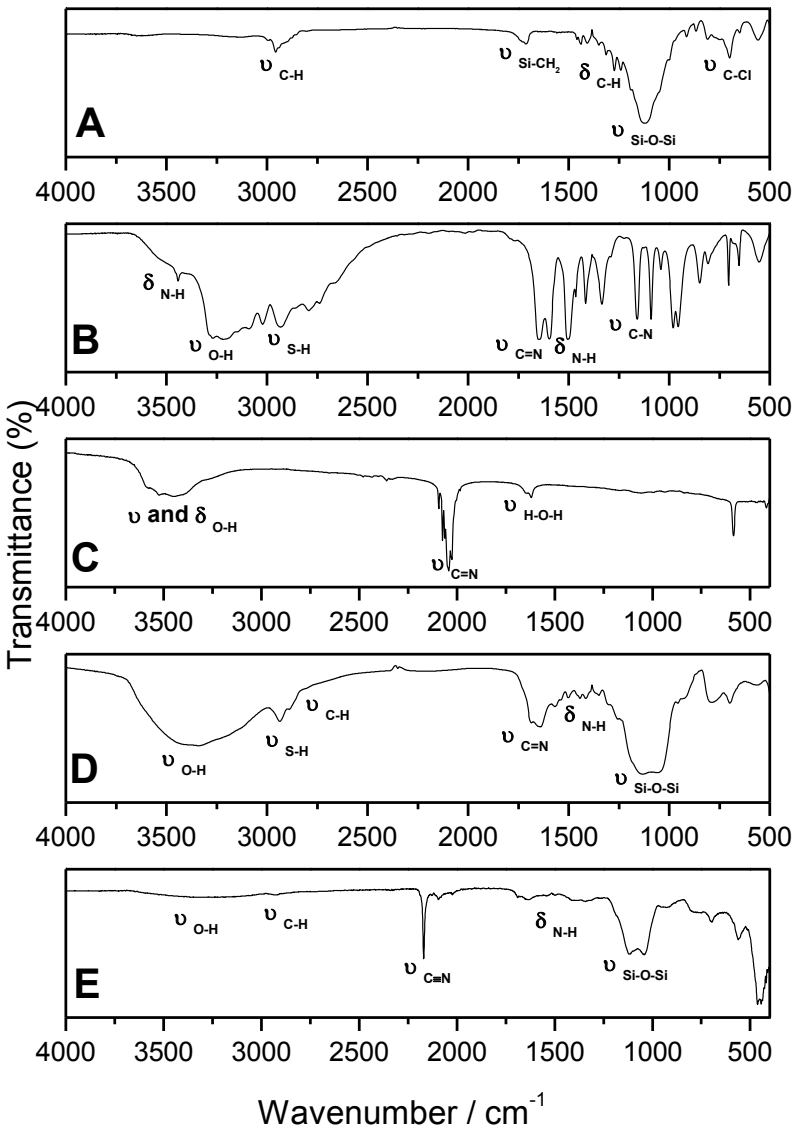

Figure 2. Spectrum in the infrared region of: (A) octa-(3-chloropropyl)silsesquioxane (S); (B) Purpald®; (C) Potassium Hexacyanoferrate (III); (D) Silsesquioxane modified with Purpald® (SP); (E) AgHSP.

Fig. 2E illustrates the infrared spectrum of AgHSP obtained after silver adsorption with SP (AgSP) and subsequent reaction with potassium hexacyanoferrate (III). The spectra (Fig. 2D) and

(Fig. 2C) showed the same peaks observed in spectrum (Fig. 2E) except for a peak at 2172 cm^{-1} found only on the curve (Fig. 2E). This peak, assigned to C≡N (υ C≡N) stretching confirms the formation of silver hexacyanoferrate composite [38] formed after reaction of the starting material AgSP with potassium hexacyanoferrate (III). This peak is 169 cm^{-1} shifted with to higher energy with relation to potassium hexacyanoferrate (Fig. 2C). This behavior is in according to one described in the literature [38] and is attributed to both the kinematic coupling that occurs when a second mass is attached to the CN unit as well as to the fact that the N lone pair is antiboding with respect to the C≡N bond [39].

AgHSP was characterized by cyclic voltammetry as shown in Fig. 3. With the voltammogram of AgHSP (20% m/m), a redox pair (peak I) was observed with a midi potential E^{θ}'= 0.64 V (ν=20 mV s^{-1}; KNO_3 1.0 M), attributed to the redox process $Fe^{(II)}(CN)_6/Fe^{(III)}(CN)_6$ of the binuclear complex formed on the material surface SP. Analogous results were reported by literature [40].

Studies on various supporting electrolytes (KNO_3, $NaNO_3$ and NH_4NO_3) for studies of cations are illustrated in Fig. 3. It was observed that the nature of the cations affected the average potential (E^{θ}') and the current intensities, but was not verified any interference of anions with exception of chloride (Cl^-).

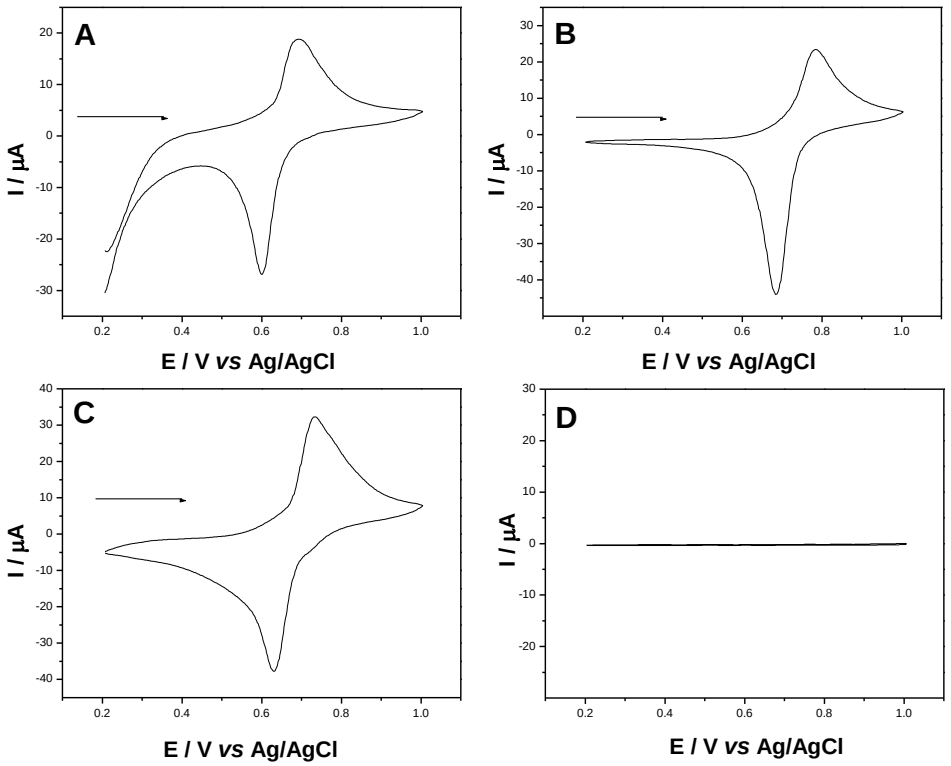

Figure 3. Cyclic voltammograms of graphite electrode modified with AgHSP: (A) $NaNO_3$, (B) KNO_3, (C) NH_4NO_3 and (D) KCl (1.0 mol L^{-1}; v = 20 mV s^{-1}; 20% (w/w)).

It was also observed that the cyclic voltammograms of AgHSP in the presence of electrolytes KNO_3, $NaNO_3$ and NH_4NO_3 (Fig. 3), showed a well-defined redox pair and that there was a shift in the average potentials (E^{θ}') to more positive potentials, in the following order: $NH_4^+ > K^+ > Na^+$, as shown in

Table 1, which are also lists the main electrochemical parameters of the compounds and their respective hydration radii.

Table 1. Relation of the diameter of hydrated cations with the electrochemical parameters of AgHSP 1.0 mol L^{-1}; v = 20 mVs^{-1}; 20%(w/w)).

Cation	[Ipa/Ipc]	($E^{\theta'}$) (V)	ΔEp [Epa-Epc]	Diameter of Hydrated Cation (nm)**
Na^+	0.53	0.64	0.09	0.36
K^+	0.58	0.73	0.10	0.24
NH_4^+	0.77	0.68	0.10	0.24

** Ref.[40]

Analogous to studies on CuHSA [29] and for being a compound analogous to Prussian blue, these materials exhibit a zeolite structure type, presenting cavities that allow the inflow and outflow of some metal ions with smaller hydration radii [41-43]. For this reason, the cations K^+ and NH_4^+ (smaller hydration radii - Table 1) diffuse more easily between these cavities, resulting in a better electrochemical response of the modified electrode. With the data presented in Table 1, it was concluded that the electrolyte of KNO_3 (K^+) showed a better voltammetric performance compared to the electrolyte NH_4NO_3 (NH_4^+), as is also observed in Fig. 3 (B) and (C)), this fact is explained by the low mobility of the cation NH_4^+ with regards to cation K^+. However, as Na^+ has a larger hydration diameter than the cavity presented by AgHSP, it hinders the redox process [40].

Fig. 3 shows only the presence of one redox pair, independently of the cations responsible for the compensation and balancing of the charges, and this redox process is related to the transition $Ag^{(I)}/Fe^{(II)}$ – $Ag^{(I)}/Fe^{(III)}$ equivalent to the second redox pair in the Prussian Blue system [40].

The nature of the anions NO_3^-, SO_4^{2-} hardly affects the redox process, however, the voltammogram (Fig. 3D) for the electrolyte KCl showed a dramatic decrease in the current and the total disappearance of the redox process of the peak, such an effect may be related to formation of AgCl, which blocks the electron transfer process at the electrode surface, similar results were also reported by Jayasri and Narayanan [40].

Fig. 4 illustrates the cyclic voltammograms obtained with different concentrations of KNO_3 (1.0×10^{-3} to 2.0 mol L^{-1}). There is a small shift in formal potential to more positive values with increasing electrolyte concentration.

Fig. 5 shows that the average formal potential values ($E^{\theta'}$) shifted linearly (R=0.998) to more positive potentials by varying the concentration of KNO_3 from 1.0×10^{-3} to 2.0 mol L^{-1}. This study enabled to see that for the graphite paste electrode modified with AgHSP, the slope line is of 53 mV per decade of concentration of potassium ions, indicating that the behavior exhibited by the electrode moves close to quasi nernstian process with the transfer of one electron [40, 44].

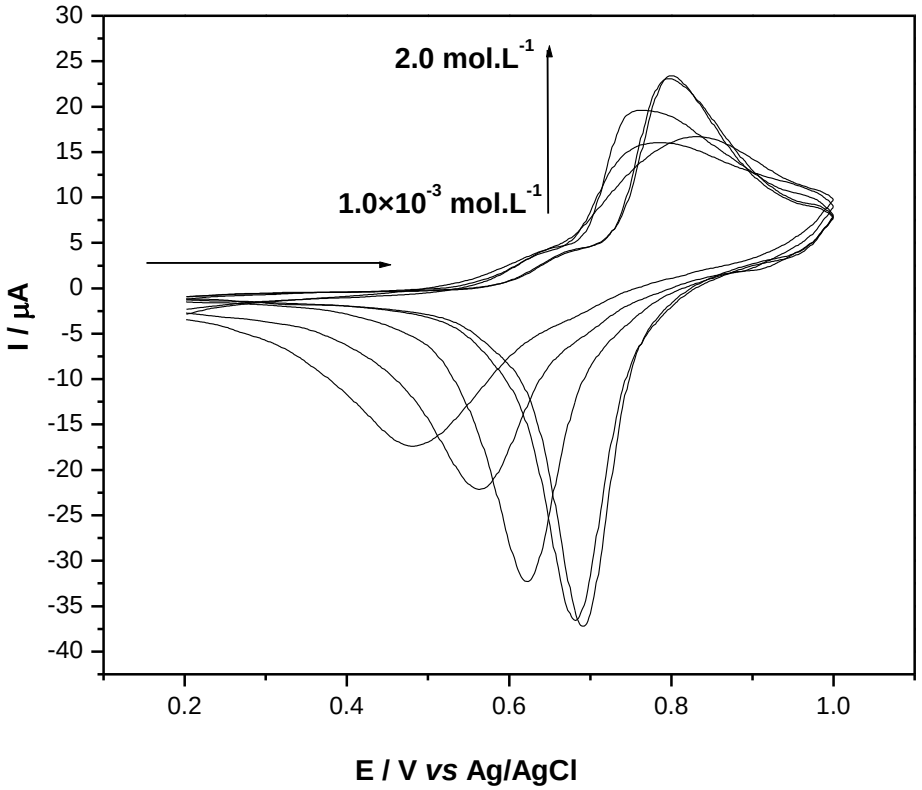

Figure 4. Cyclic voltammograms of the graphite paste electrode modified with AgHSP at different concentrations (KNO_3; v = 30 mV s^{-1}; 20% (w/w)).

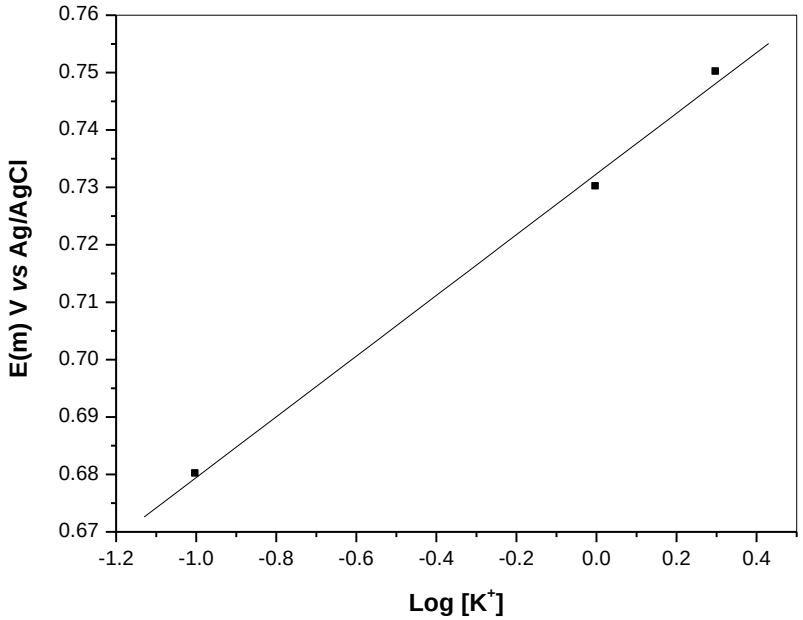

Figure 5. Average potential (E^{θ}') of graphite paste modified with AgHSP as a function of KNO_3 concentration.

For the calculations of the aforementioned line slope the voltammograms corresponding to concentrations of 0.1 to 2.0 mol L^{-1} were used, as in this range there were more well-defined redox processes, as shown in Table 2.

Table 2. Electrochemical parameters of AgHSP at different electrolyte concentrations (KNO_3; v = 30 mVs^{-1}; 20%(w/w)).

Concentration (mol L^{-1})	[Ipa/Ipc]	($E^{\theta'}$) (V)	ΔEp (V) [Epa-Epc]
1.0×10^{-3}	1.83	0.66	0.35
1.0×10^{-2}	1.05	0.66	0.21
1.0×10^{-1}	0.68	0.69	0.14
1.00	0.67	0.73	0.12
2.00	0.65	0.75	0.11

With the results presented in this study, the concentration of 0.1 mol L^{-1} was determined as the best concentration of the electrolyte KNO_3 due to the good voltammetric performance presented.

Fig. 6 shows the cyclic voltammogram at different pH values (2-7). It was observed that at pHs 2 to 7 there is no significant change in the peak current and there is not shift of the average peak potential, which can afirm that the hydrogen ion concentration does not affect the electrochemical process. However, at pH 2 there was the appearance of two new redox processes.

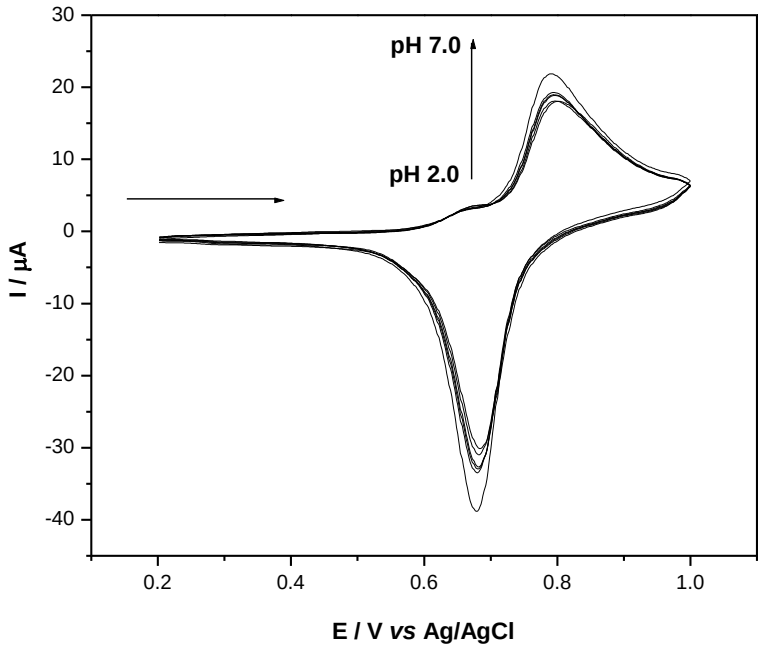

Figure 6. Cyclic voltammograms of graphite paste electrode modified with AgHSP at different pH values (v =30 mV s^{-1}; KNO_3 1.0 mol L^{-1}; 20% (w/w)).

Fig. 7 illustrates the cyclic voltammogram of AgHSP at different scan rates (10 to 100 mVs^{-1}), it was observed that by increasing the scan rate there is an increased anodic peak current and also a small shift of the average potential to more positive values [40]. It was observable a appearance of a shoulder at 0.67 V. This suggest an existence of anothers species of fast oxidation kinetic process. Table 3 shows the main electrochemical parameters of AgHSP for different scan rates.

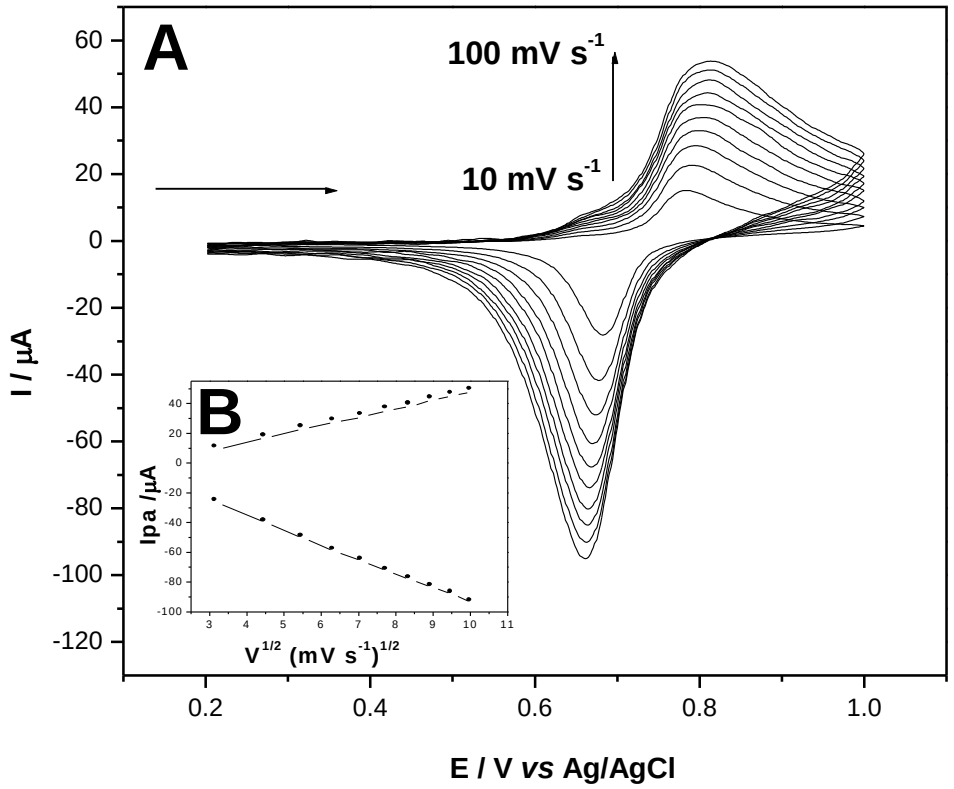

Figure 7. (A) Cyclic voltammograms of AgHSP at different scan rates (KNO_3 1.0 mol L^{-1}; 20% (w/w)) and (B) dependence of peak current intensity (anodic and cathodic) as a function of scan rate.

Table 3. Electrochemical parameters of AgHSP at different scan rates (KNO_3 1.0 mol L^{-1}; pH 7.0; 20%(w/w)).

Scan rate ($mV\ s^{-1}$)	[Ipa/Ipc]	($E^{0'}$) (V)	ΔEp (V) [Epa-Epc]
10	0.42	0.73	0.10
20	0.47	0.73	0.11
30	0.49	0.73	0.12
40	0.49	0.73	0.12
50	0.50	0.73	0.13
60	0.51	0.73	0.14
70	0.51	0.73	0.14
80	0.53	0.73	0.14
90	0.54	0.73	0.14
100	0.53	0.73	0.15

Furthermore, as illustrated by Fig. 7, the current intensities of the anodic (R=0.999) and cathodic catódico (R=0.989 peak) (Ipa and Ipc) have a linear relationship with the square root of the scan rate, thus characterizing a diffusional process [44].

3.1. Electroanalytical application of composite AgHSP electrocatalytic oxidation of Sodium sulfite

Fig. 8 illustrates the voltammetric behavior of the graphite paste electrode modified with AgHSP for the electro-oxidation of sodium sulfite in 1.0 mol L^{-1} KNO_3. The graphite paste unmodified electrode in a solution of KNO_3 1.0 mol L^{-1} in the absence (curve A) and presence of sodium sulfite (curve D) did not show a redox pair in the potential range studied between 0.2 and 1.0 V. After the addition of sodium sulfite there was an increase in the anodic peak current intensity (curve C) when compared with the graphite paste electrode modified with AgHSP in absence of sulfite (curve B). There was an increase in the anodic current intensity of the peak at 0.77 V and a small shift to more negative potentials. Thus, it was determined that with de adding aliquots of the sodium sulfite, the analite was oxidized by an electrocatalyst oxidation process on the electrode surface.

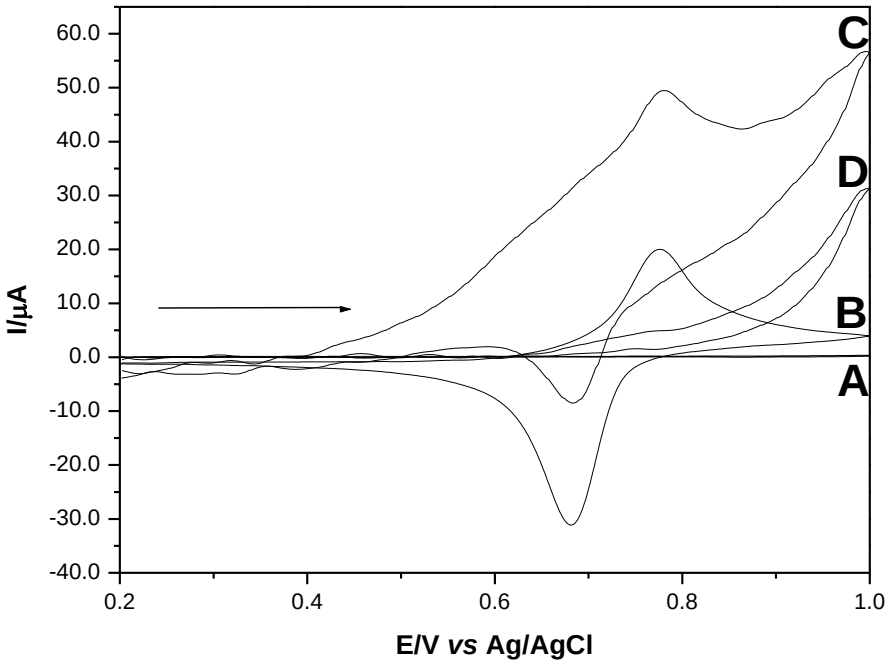

Figure 8. Cyclic voltammograms: (A) of the graphite paste electrode; (B) graphite paste electrode modified with AgHSP; (C) graphite paste electrode modified with AgHSP and 1.0×10^{-3} mol L^{-1} of sulfite; (D) graphite paste electrode and 1.0×10^{-3} mol L^{-1} of sulfite (KNO_3 1.0 mol L^{-1}; 20mV s^{-1}; 20%(m/m)).

The electrocatalytic oxidation of sulfite occurs as follows: Fe^{3+} produced during anodic scan, chemically oxidize the molecule sulfite when it is reduced to Fe^{2+}, which will again be electrochemically oxidized to Fe^{3+}.

To this system, the electrocatalytic process can also be represented according to the equations 1 and 2:

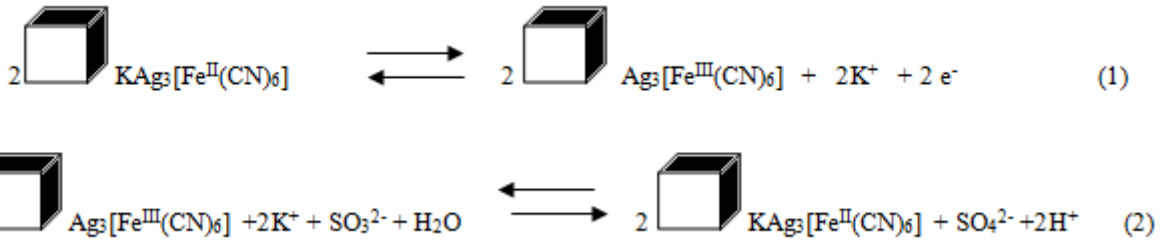

Thus sulfite is oxidized at the electrode surface, and this process occurs in the potential of 0.77 V. The oxidation process does not occur in this potential when is used glassy carbon electrode or unmodified carbon paste (Fig. 8D). The peak potential is not affected by the concentration of sulfite and the catalytic current is also linear with the square root of scan rate. The behavior of electrochemical oxidation of sulfite in the AgHSP. Fig. 10 illustrates the analytical curve used to determinate sodium sulfite. The modified electrode showed a linear response from 7.0×10^{-5} to 1.0×10^{-3} mol L^{-1} with the corresponding equation Y(μA) = 18.05 + 29.983×10^{3} [sulfite], and a correlation coefficient of r=0.999. The method showed a detection limit of 0.115×10^{-4} mol L^{-1} with a relative standard deviation of ± 4% (*n* = 3) and amperometric sensitivity of 29.983×10^{-3}A mol L^{-1}.

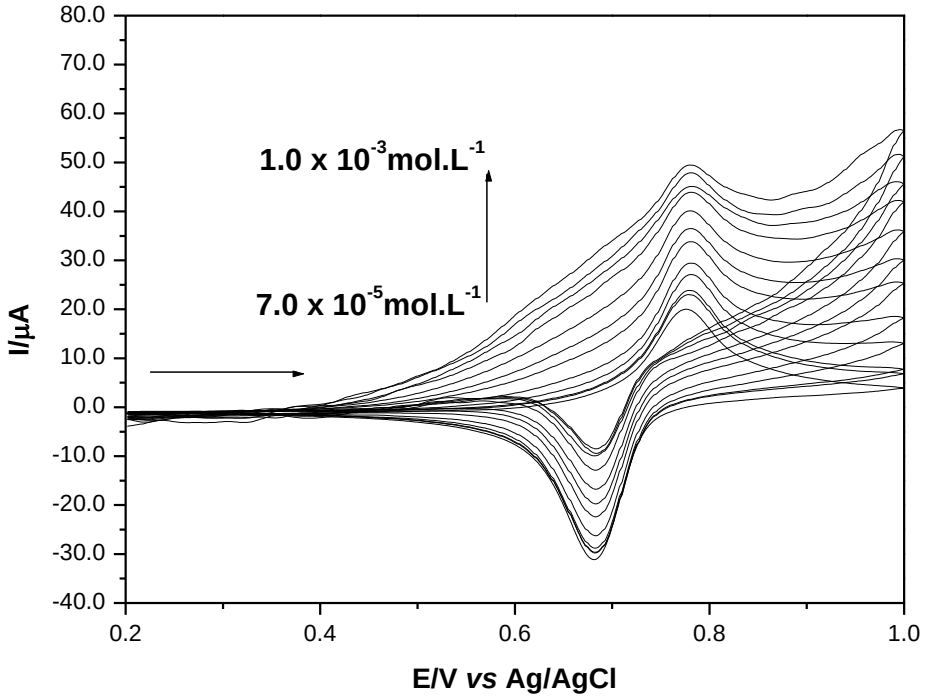

Figure 9. Cyclic voltammograms of applications of various concentrations of sodium sulfite graphite paste electrode modified with AgHSP (KNO_3 1.0 $molL^{-1}$; 20 mVs^{-1}; 20% (m/m)).

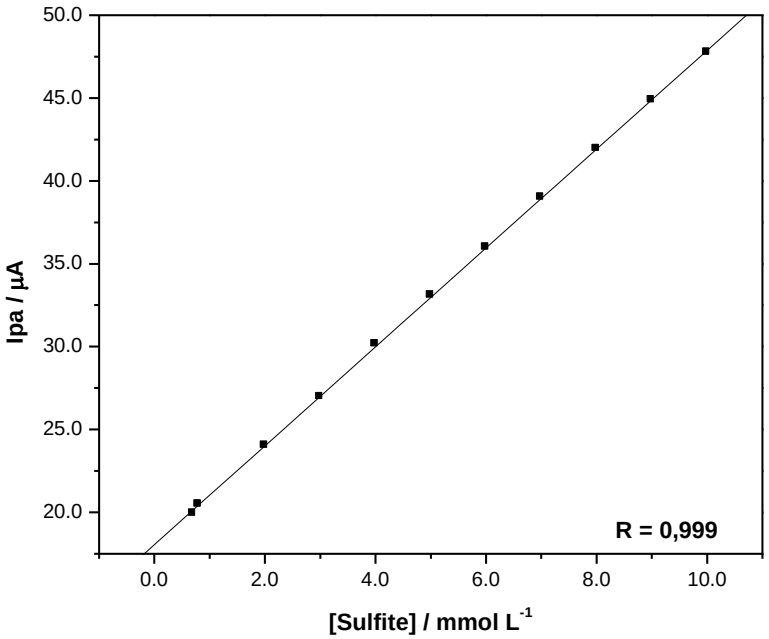

Figure 10. Analytical curve for the determination of sodium sulfite using the graphite paste electrode modified with AgHSP (KNO_3 1.0 mol L^{-1}; 20 mV s^{-1}; 20%(m/m)).

4. CONCLUSION

A preliminary characterization by FTIR and cyclic voltammetry of a composite formed by interaction of a octa (3-chloropropyl)octasilsesquioxane and Purpald®, after silver adsorption and subsequent reaction of hexacyanoferrate (AgHSP) was conducted using graphite paste electrode

The cyclic voltammogram of the modified graphite paste electrode with AgHSP, showed one redox couple with formal potential ($E^{\theta'}$) = 0.64 V (ν=20 mV s^{-1}; KNO_3 1.0 M), attributed to the redox process $Fe^{(II)}(CN)_6/Fe^{(III)}(CN)_6$. The redox couple presents electrocatalytic property for sulfite. Quantitation in millimolar range of sulfite in pharmaceutical can be achieved using graphite paste electrode modified with AgHSP. The modified electrode showed a linear response from 7.0×10^{-5} to 1.0×10^{-3} mol L^{-1} with the corresponding equation Y(μA) = 18.05 + 29.983×10^{3} [sulfite], and a correlation coefficient of r=0.999. The method showed a detection limit of 0.115×10^{-4} mol L^{-1} with a relative standard deviation of ± 4% (n = 3) and amperometric sensitivity of 29.983×10^{-3}A mol L^{-1}.Additionaly the modified electrode showed a excellent stability and good reproducibility during experiments.

ACKNOWLEDGEMENTS
The authors are grateful for Fundação de Amparo à Pesquisa do Estado de São Paulo (FAPESP - Procs. 2012/05438-1 and 2012/11306-0) and Coordenação de Aperfeiçoamento de Pessoal de Nível Superior (CAPES) for financial support..

References

1. R. H. Baney, M. Itoh, A. Sakakibara, T. Suzukit, *Chem. Rev.*, 95 (1995) 1409.
2. S. W. Kuo, F. C. Chang, *Prog. Polym. Sci.*, 36 (2011) 1649.
3. D. Gnanasekaran, K. Madhavan, B. S. R. Reddy, *J. Sci. Ind. Res.*, 68 (2009) 437.
4. D. B. Cordes, P. D. Lickiss, F. Rataboul, *Chem. Rev.*, 110 (2010) 2081.
5. D. Xu, L. S. Loo, K. Wang, *J. Appl. Polym. Sci.*, 122 (2011) 427.
6. C. Ni, G. Ni, L. Zhang, J. Mi, B. Yao, C. Zhu, *J. Coll. Int. Sci.*, 362 (2011) 94.
7. T. A. Tereshchenko, *Polym. Sci.*, 50 (2008) 249.
8. A. Provatas, M. Luft, J. C. Mu, A. H. White, J. G. Matisons, B. W. Skelton, *J. Organomet. Chem.*, 565 (1998) 159.
9. E. A. Quadrelli, J. M. Basset, *Coord. Chem. Rev.*, 254 (2010) 707.
10. X. Zhang, J. Sun, S. Fang, X. Han, Y. Li, C. Zhang, *J. Appl. Polym. Sci.*, 122 (2011) 296.
11. M. Handke, A. Kowalewska, *Spectrochim. Acta, Part A: Mol. Biomol. Spectros.*, 79 (2011) 749.
12. S. Gabriel Junior, Preparação, caracterização e aplicações eletroanalíticas de silsesquioxanos e dendrímeros modificados suportados na superfície da sílica gel. Dissertação (Mestrado) – Faculdade de Engenharia, Universidade Estadual Paulista "Júlio de Mesquita Filho", Ilha Solteira (2010).
13. L. A. Soares, T. F. S. Da Silveira, D. R. Silvestrini, U. O. Bicalho, D. R. Do Carmo, *Int. J. Chem.*, 5 (2013) 39.
14. D. R. Do Carmo, L. L. Paim, *Mater. Res.*, 16 (2013) 164.
15. N. L. Dias Filho, R. M. Costa, M. S. Schultz, *Inorg. Chim. Acta*, 361 (2008) 2314.
16. G. Li, L. Wang, H. Ni, C. U. Pittman Junior, *J. Organomet. Chem.*, 11 (2001) 123.
17. L. A. Soares, Propriedades Analíticas e Eletroanalíticas de um Silsesquioxano Nanoestruturado Organofuncionalizado. Dissertação (Mestrado) – Faculdade de Engenharia, Universidade Estadual

Paulista "Júlio de Mesquita Filho", Ilha Solteira (2011).
18. R. M. Laine, M. F. Roll, *Macromolecules*, 44 (2011) 1073.
19. H. C. L. Abbenhuis, *Chem. – Eur. J.*, 6 (2000) 25.
20. A. Fina, D. Tabuani, F. Carniato, A. Frache, E. Boccaleri, G. Camino, *Thermochim. Acta*, 440 (2006) 36.
21. T. F. S. Da Silveira, D. R. Silvestrini, U. O. Bicalho, D. R. Do Carmo, *Int. J. Electrochem. Sci.*, 8 (2013) 872.
22. D. R. Do Carmo, L. L. Paim, D. R. Silvestrini, A. C. De Sá, U. O. Bicalho, N. R. Stradiotto, *Int. J. Electrochem. Sci.*, 6 (2011) 1175.
23. M. Morán, C. M. Casado, I. Cuadrado, *Organometallics*, 12 (1993) 4327.
24. H. W. Ro, E. S. Park, C. L. Soles, D. Y. Yoon, *Chem. Mater.*, 22 (2010) 1330.
25. E. Devaux, M. Rochery, S. Bourbigot, *Fire Mater.*, 26 (2002) 149.
26. D. A. Wann, R. J. Less, F. Rataboul, P. D. McCaffrey, A. M. Reilly, H. E. Robertson, P. D. Lickiss, D. W. H. Rankin, *Organometallics*, 27 (2008) 4183.
27. J. Chojnowski, W. Fortuniak, P. Rościszewski, W. Werel, J. Łukasiak, W. Kamysz, R. Hałasa, *J. Inorg. Organomet. Polym. Mater.*, 16 (2006) 219.
28. D. R. Do Carmo, L. L. Paim, N. R. Stradiotto, *Mater. Res. Bull.* 47 (2012) 1028.
29. L. A. Soares, T. F. S. Da Silveira, D. R. Silvestrini, U. O. Bicalho, N. L. Dias Filho, D. R. Do Carmo, *Int. J. Electrochem. Sci.*, 8 (2013) 4654.
30. I. Willner, E. Katz, *Angew. Chem., Int. Ed.*, 39 (2000) 1180.
31. R. W. Murray, Chemically Modified Electrodes. Bard A J, (ed). Electroanalytical Chemistry, Marcel Dekker, New York, 1984.
32. A. K. Sen, R. N. Singh, R. N. Handa, S. N. Dubey, P. J. Squattrito, *J. Mol. Struct.*, 470 (1998) 61.
33. D. Pearson, The Chemical Analysis of Foods, Churchill Livingstone: Edinburgh, London and New York, 1976.
34. J. G. Muller, R. P. Hickerson, R. J. Perez, C. Burrows, *J. Am. Chem. Soc.*, 119 (1997) 1501.
35. Z. Meng, N. Sang, B. Zhang, *Bull. Environ. Contam. Toxicol.*, 69 (2002) 257.
36. D. R. Do Carmo, G. R. Castro, M. A. U. Martines, N. L. Dias Filho, N. R. Stradiotto, *Mater. Res. Bull.*, 43 (2008) 3286.
37. R. M. Silverstein, F. X. Welbster, Spectrometric identification of organic compounds. John Wiley & Sons, New York, 1996.
38. S. B. Moon, A. Xidis,V. D. Neff, *J. Phys. Chem.*, 97 (1993) 1634.
39. K. R. Karlin, *Prog. Inorg.* Chem., 45 (1997) 288.
40. D. Jayasri, S. Narayanan, *Sens. Actuators, B*, 119 (2006) 135.
41. M. A. Maliki, P. J. Kulesza, *Electroanalysis*, 6 (1996) 113.
42. S. S. Narayanan, F. Scholz, *Electroanalysis*, 11 (1999) 465.
43. M. B. Soto, F. Scholz, *J. Electroanal. Chem.*, 528 (2002) 27.
44. A. L. Bard, L. R. Faulkner, Electrochemical methods: fundamentals and Applications. John Wiley & Sons, New York, 1980.